

# Planar coupling to high-Q lithium niobate disk resonators

G. Nunzi Conti,<sup>1,\*</sup> S. Berneschi,<sup>1,2</sup> F. Cosi,<sup>1</sup> S. Pelli,<sup>1</sup> S. Soria,<sup>1</sup> G. C. Righini,<sup>1</sup>  
M. Dispenza,<sup>3</sup> and A. Secchi<sup>3</sup>

<sup>1</sup>“NelloCarrara” Institute of Applied Physics, IFAC-CNR, Via Madonna del Piano 10,  
50019 Sesto Fiorentino, Firenze, Italy

<sup>2</sup>Museo Storico della Fisica e Centro Studi e Ricerche “Enrico Fermi”, Piazza del Viminale 2, 00184 Roma, Italy

<sup>3</sup>Microelectronics & Photonics Dept., SELEX Sistemi Integrati SpA, Via Tiburtina, Km 12,400 00131, Roma, Italy  
[\\*g.nunziconti@ifac.cnr.it](mailto:g.nunziconti@ifac.cnr.it)

**Abstract:** We demonstrate optical coupling to high-Q lithium niobate disks from an integrated lithium niobate waveguide. The waveguides are made by proton exchange in X-cut lithium niobate substrate. The disks with diameter of 4.7 mm and thickness of 1 mm are made from commercial Z-cut lithium niobate wafers by polishing the edges into a spheroidal profile. Both resonance linewidth and cavity ringdown measurements were performed to calculate the Q factor of the resonator, which is in excess of  $10^8$ . Planar coupling represents the most promising technique for practical applications of whispering gallery mode resonators.

©2011 Optical Society of America

**OCIS codes:** (230.5750) Resonators; (140.4780) Optical resonators; (130.3730) Lithium niobate; (130.0130) Integrated optics; (230.7390) Waveguide, planar.

---

## References and links

1. V. S. Ilchenko, A. A. Savchenkov, A. B. Matsko, and L. Maleki, “Nonlinear optics and crystalline whispering gallery mode cavities,” *Phys. Rev. Lett.* **92**(4), 043903 (2004).
2. A. A. Savchenkov, V. S. Ilchenko, A. B. Matsko, and L. Maleki, “Kilohertz optical resonances in dielectric crystal cavities,” *Phys. Rev. A* **70**(5), 051804 (2004).
3. L. Maleki, V. S. Ilchenko, A. A. Savchenkov, and A. B. Matsko, “Crystalline Whispering Gallery Mode Resonators in Optics and Photonics” in *Practical Applications of Microresonators in Optics and Photonics*, A. B. Matsko, ed. (CRC Press, Boca Raton, FL, 2009).
4. A. Chiasera, Y. Dumeige, P. Féron, M. Ferrari, Y. Jestin, G. Nunzi Conti, S. Pelli, S. Soria, and G. C. Righini, “Spherical Whispering-Gallery-Mode Microresonators,” *Laser Photon. Rev.* **4**(3), 457–482 (2010).
5. G. C. Righini, M. Brenci, A. Chiasera, P. Feron, M. Ferrari, G. Nunzi Conti, and S. Pelli, “Whispering gallery mode resonators for microlasers and microsensors,” *Proc. SPIE* **6029**, 602903, 602903-8 (2006).
6. L. Maleki, and A. B. Matsko, “Lithium Niobate Whispering Gallery Mode Resonators: Applications and Fundamental Studies” in *Ferroelectric Crystals for Photonics Applications*, P. Ferraro, S. Grilli, P. De Natale, ed. (Springer-Verlag, Berlin Heidelberg, 2009).
7. J. U. Fürst, D. V. Strekalov, D. Elser, M. Lassen, U. L. Andersen, C. Marquardt, and G. Leuchs, “Naturally phase-matched second-harmonic generation in a whispering-gallery-mode resonator,” *Phys. Rev. Lett.* **104**(15), 153901 (2010).
8. B. E. Little, J.-P. Laine, D. R. Lim, H. A. Haus, L. C. Kimerling, and S. T. Chu, “Pedestal antiresonant reflecting waveguides for robust coupling to microsphere resonators and for microphotonic circuits,” *Opt. Lett.* **25**(1), 73–75 (2000).
9. Y. Panitchob, G. S. Murugan, M. N. Zervas, P. Horak, S. Berneschi, S. Pelli, G. Nunzi Conti, and J. S. Wilkinson, “Whispering gallery mode spectra of channel waveguide coupled microspheres,” *Opt. Express* **16**(15), 11066–11076 (2008), <http://www.opticsinfobase.org/oe/issue.cfm?volume=16&issue=15>.
10. X. F. Cao, R. V. Ramaswamy, and R. Srivastava, “Characterization of Annealed Proton Exchanged LiNbO3 Waveguides for Nonlinear Frequency Conversion,” *J. Lightwave Technol.* **10**(9), 1302–1313 (1992).
11. Y. Dumeige, S. Trebaol, L. Ghisa, T. K. N. Nguyễn, H. Tavernier, and P. Féron, “Determination of coupling regime of high-Q resonators and optical gain of highly selective amplifiers,” *J. Opt. Soc. Am. B* **25**(12), 2073–2080 (2008).
12. B. E. Little, J.-P. Laine, and H. A. Haus, “Analytic Theory of Coupling from Tapered Fibers and Half-Blocks into Microsphere Resonators,” *J. Lightwave Technol.* **17**(4), 704–715 (1999).

13. G. S. Murugan, Y. Panitchob, E. J. Tull, P. N. Bartlett, D. W. Hewak, M. N. Zervas, and J. S. Wilkinson, "Position-dependent coupling between a channel waveguide and a distorted microsphere resonator," *J. Appl. Phys.* **107**(5), 053105 (2010).
  14. M. L. Gorodetsky, and V. S. Ilchenko, "Optical microsphere resonators: optimal coupling to high- $Q$  whispering-gallery modes," *J. Opt. Soc. Am. B* **16**(1), 147–154 (1999).
- 

## 1. Introduction

Crystalline Whispering Gallery Mode (WGM) optical resonators have gained increasing attention since the possibility of getting very high  $Q$  factors ( $Q > 10^8$ ) was demonstrated in various crystals [1,2]. Both for practical applications as well as for fundamental studies, some useful properties specific of crystals can provide additional advantages to these resonators [3] as compared to the amorphous counterparts [4]. For instance ultimate  $Q$  factors of microspheres made of fused silica in the 1.55  $\mu\text{m}$  window rapidly decrease in atmosphere due to diffusion of water into the material [5] while a number of crystals do not absorb moisture. In general high-purity crystals theoretically have a perfect lattice without inclusions and inhomogeneities that are always present in amorphous materials and therefore they typically have very low intrinsic absorption of light within their transparency window. Enhanced non linear or electro-optical properties may play an additional role for the implementation of high performance devices. This is the case of resonators made in lithium niobate that can be used for the realization of a number of specific components including single and multi-order tunable filters, electro-optic modulators, or frequency converters [6,7].

For practical application of WGM resonators the crucial issue is yet the implementation of an efficient and robust coupling scheme. Coupling through a high index prism or an integrated surface waveguide definitely represents the most promising approaches. Indeed, prism coupling technique, which involves free space beams, is typically used to efficiently couple light in and out of a crystalline resonator [3]. Planar coupling to low  $Q$  glass microspheres has been demonstrated [8,9], but in this paper we present the first demonstration of planar coupling to high  $Q$  crystalline WGM resonators.

We implemented optical coupling to high- $Q$  lithium niobate disks from a fiber pigtailed integrated lithium niobate waveguide, realizing a system which is all in guided optics architecture. The waveguides are made by proton exchange in X-cut lithium niobate while the high- $Q$  disks are made from commercial Z-cut lithium niobate wafers by polishing the edges into a spheroidal profile.

## 2. Disk and waveguide fabrication

Lithium niobate disks of 4.7 mm in diameter were made from commercial 3" x 1 mm thick Z-cut lithium niobate wafers by core drilling a cylinder and thereafter polishing the edge into a spheroidal shape. We have optimized the polishing procedure of crystalline disks using a home-made lapping station. The almost spherical profile is obtained through a rotational stage whose pivot point can be finely adjusted. The polishing protocol is divided in six successive steps starting with an initial two-step grinding phase (disks with abrasive size of 12 and 9 microns) which is followed by a four-step finer polishing phase, based on polycrystalline diamond suspensions with decreasing grit sizes (3, 1, 0.25, and 0.05 microns, respectively). After each step a rather critical cleaning procedure using organic solvents has been implemented. Because of the large disk thickness (1 mm) the modal structure of the resonator is, for all practical purpose, identical to that of a spheroid.

Waveguides in X-cut lithium niobate wafers were fabricated by thermal annealing proton exchange (TAPE). Lithium niobate TAPE channels are widely adopted waveguides, thanks to their low propagation loss, stability and electro-optic performance. The manufacturing of TAPE waveguides is a two-stage process, the proton exchange (PE) and then the thermal annealing. The lithium niobate uniaxial crystal substrate is first immersed in a benzoic acid bath at a fixed temperature, typically 190°C. The protons in the bath and the lithium ions in the crystal are exchanged through a  $\text{SiO}_2$  mask opening (6  $\mu\text{m}$  wide in our case), thereby

increasing the proton concentration and reducing the lithium concentration in the crystal. The PE process in benzoic acid yields an increase of the  $\text{LiNbO}_3$  extraordinary refractive index, while the ordinary index remains almost unchanged. Moreover, there is a reduction of the electro-optic coefficient, and propagation losses increase. Experimental measurements show that an almost rectangular channel is formed at the end of the PE process. In the second stage the protons are redistributed inside the substrate by an annealing process, which restores both the electro-optic coefficient and the optical transmission. After the thermal annealing, a channel waveguide with diffused index profile is obtained and the extraordinary refractive index in the transverse plane can be expressed by an analytical function [10]. As the ordinary index still remains unchanged only the TE mode can be guided. With a lithium niobate bulk extraordinary index at 1550 nm equal to 2.13 and a maximum refractive index change at the surface of 0.04, the calculated waveguide effective index of the fundamental TE mode is 2.143. The measured insertion loss of a 5 cm long fiber pigtailed waveguide is 3 dB.

### 3. Experimental setup

The experimental setup for waveguide coupling and Q factor measurement is sketched in Fig. 1a. A fiber pigtailed tunable external cavity laser operating around 1550 nm (Tunics Plus) and with a linewidth of 300 KHz is used as light source. The laser can be finely and continuously swept in wavelength by a few GHz and an external signal like a symmetric triangular wave can be applied to modulate the wavelength with frequencies up to 10 KHz. With a variable attenuator and a polarization controller both the power and polarization state of the light coupled to the fiber pigtailed lithium niobate waveguide can be controlled. The transmission at the output of the waveguide is monitored using an InGaAs detector connected to an oscilloscope. We used a 10 MHz bandwidth (Thorlabs PDA 400) detector for slow scanning and a 1 ns rise time (New Focus 1623) detector for fast scanning. Slow or fast scanning depends on the time needed for the laser to ‘cross’ the resonance as compared to the cavity photon lifetime  $\tau$  [11]. The disk position relative to the waveguide can be controlled using a 3 axis translational stage with sub-micrometer resolution (10 nm). During the measurements the disk was placed and kept in contact with the lithium niobate substrate in order to improve the stability of the system. The coupling efficiency from the waveguide to the microdisk could still be changed by laterally displacing the resonator, thus varying the distance  $d$  between the center of the waveguide and the disk-substrate contact point. Figure 1b shows a sketch of a section of the disk-waveguide system perpendicular to the direction of light propagation, including crystal axis orientation and modes polarization. A photo of the system is presented in Fig. 2, where both the 5 cm long fiber pigtailed waveguide and the lithium niobate disk, which is mounted on an aluminum holder, can be seen.

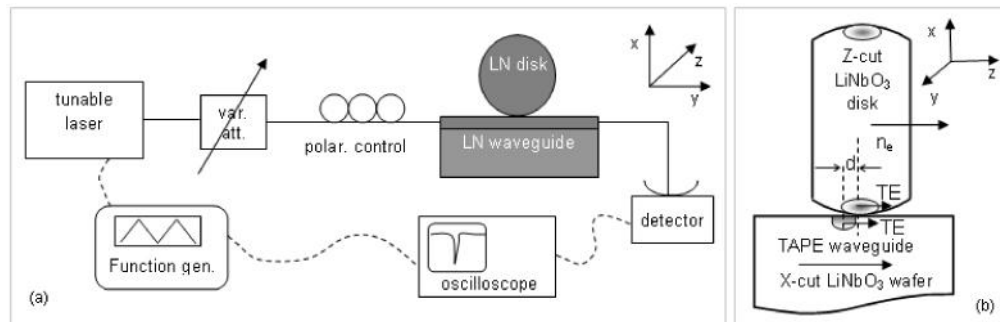


Fig. 1. (a) Sketch of the experimental setup with lateral view of the waveguide and of the disk. (b) Section (perpendicular to the waveguide) of the disk-waveguide system, including crystal axis orientation and waveguide and WG modes polarization.

#### 4. Waveguide to disk coupling: results and discussion

We were able to successfully couple light into the resonator from the waveguide as shown in the transmission spectra presented in Fig. 3. The whispering gallery modes were detected by slowly modulating (108 Hz) with a triangular wave the laser frequency of about 3 GHz around 1550 nm (scanning speed = 0.65 MHz/ $\mu$ s). As the laser emission frequency matches a disk WGM, a dip appears in the signal transmitted through the waveguide and the Q factor can be calculated from the resonance width  $\delta\nu$  ( $Q=v/\delta\nu$ ). No additional losses outside resonance were introduced in the waveguide transmission when the disk was in contact. The set of WGM spectra in Fig. 3a were collected for different  $d$  values, i.e. by laterally displacing the disk along the z direction to various positions across the waveguide. We observe that a number of different modes can be excited and that, increasing the distance  $d$ , we reduce the coupling coefficient and the resonance contrast, till finally coupling is no more observed for translations beyond 16  $\mu$ m. We point out that for the ‘fundamental’ mode with radial number  $n = 1$  and highest azimuthal number  $l$  the half width at half maximum (HWHM) in the lateral direction is indeed about 16  $\mu$ m [4]. Because of the large disk curvature coupling still occurs for  $d$  values larger than the actual waveguide halfwidth (3  $\mu$ m) i.e. when the disk point of contact with the lithium niobate substrate is outside the waveguide.

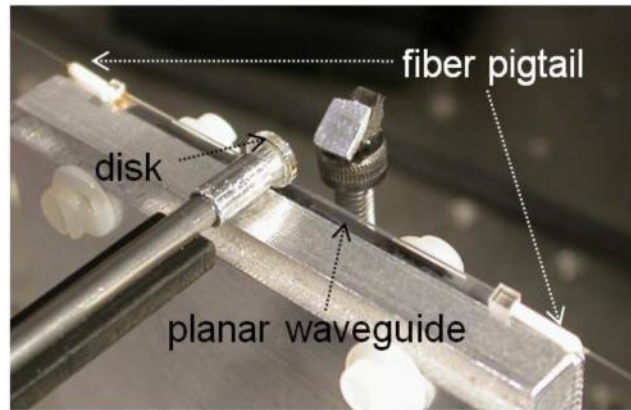


Fig. 2. Photo showing the lithium niobate disk positioned on the 5 cm long fiber pigtailed lithium niobate waveguide.

Highest coupling with a maximum contrast of about 33%, as shown in Fig. 3b, was instead observed when the disk was aligned with the waveguide ( $d=0$ ). The corresponding resonance Q factors are typically in excess of  $10^7$ . The limited efficiency of the coupling is also due to the fact that, though mode polarizations are matched (TE), there is a slight mismatch between the waveguide fundamental mode effective index ( $2.143\pm 0.001$ ) and the disk WG ‘fundamental’ mode index ( $2.122\pm 0.002$ ). It is well known that propagation constants mismatch strongly reduces the coupling coefficient [12].

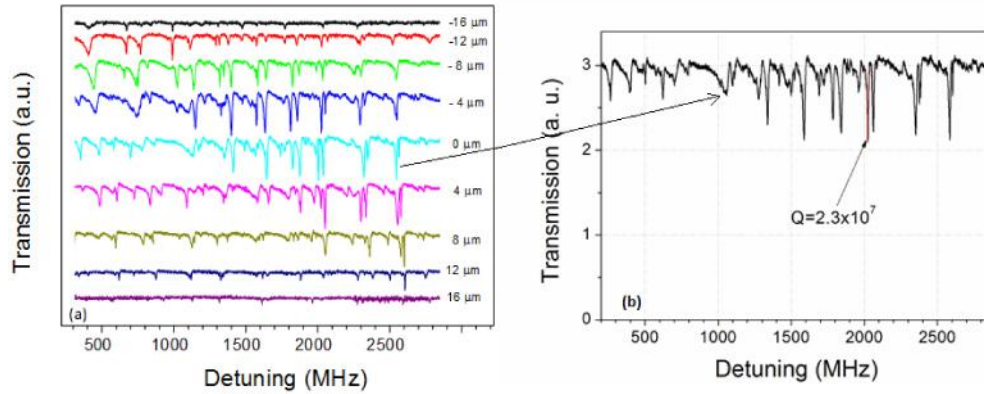


Fig. 3. (a) Resonator WGM spectra around 1550 nm (3 GHz scan) collected by laterally displacing the disk along various positions across the waveguide. (b) Spectrum of resonances taken with the disk aligned with the waveguide center ( $d=0$ ) showing a maximum contrast of 33%.

The disk resonances in Fig. 3 were collected with a slow scan of about 3 GHz, which is about a third of the resonator FSR (9.5 GHz, mode spacing for same  $n$  number and  $\Delta l=1$ ). The rather dense and complex spectra of excited WGMs also appear because of the non-perfect sphericity of the disk resonator rim, which removes the degeneracy versus the polar  $m$  number [4]. In practice the assignment of the set of  $l$ ,  $n$  and  $m$  numbers for the various resonances positions, as done in Ref. [9], would be much more critical mainly because of the much larger size of the resonators (with  $l$  values in excess of  $2 \times 10^4$ ). In addition Fig. 3a shows that negative lateral  $z$  displacements yield a different spectrum with respect to  $z$  displacements similarly to the case of Ref. [13]. Here asymmetrical behavior is also related to the different shape between the two disk hemispheres separated by the equatorial plane, as one is slightly prolate (with eccentricity  $e \approx 0.3\%$  in the negative direction), and the other slightly oblate ( $e \approx -0.2\%$ ). The observed minimum separation between WGMs, which is of the order of 20 MHz, can then be explained according to the relation  $\Delta v_{\Delta m=1} = ev/l$ , which accounts for the splitting between modes with successive polar number  $m$  [4].

As we previously stated, the planar coupler allows a stable collection of disk resonances when moving the disk away from the waveguide center. In this way we can move further in the undercoupled regime with a reduced resonance dip contrast till the measured Q factor approaches the intrinsic disk Q value [5,14]. We were thus able to obtain the lithium niobate disk Q factor by performing measurements both in the stationary regime with a slow scan as well as with ringdown technique and faster scan [11]. Figure 4a shows a low contrast (6%) resonance – obtained with low scanning speed – and the corresponding Lorentzian fit from which the Q value can be obtained ( $Q = v/\delta v$ ). Figure 4b shows instead the ringing phenomenon for the same resonance under a ten time faster scan (scanning speed = 6.8 MHz/ $\mu$ s). In this case the decay constant  $\tau_f$  of the beat note signal corresponds to the amplitude decay of the resonator field and the Q factor is obtained from the relation  $Q = \pi v \tau_f = 2\pi v \tau$ . In both cases we obtained the same Q factor value of  $1.3 (\pm 0.05) \times 10^8$ , which corresponds to the state of the art for lithium niobate disk resonators [6].

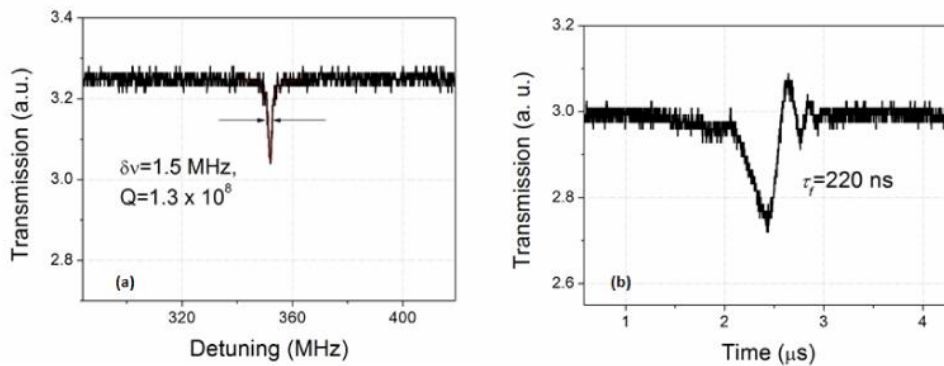


Fig. 4. (a) Lithium niobate disk Q factor measurement in stationary condition (slow scanning), i.e. from resonance linewidth, and (b) cavity ringdown measurement of the same resonance (fast scanning).

## 5. Conclusions

Optical coupling from a fiber pigtailed integrated lithium niobate waveguide to high-Q WGM lithium niobate disks was demonstrated. The waveguides are made by proton exchange in X-cut lithium niobate wafers. The WGM disk resonators with diameters of 4.7 mm are made from commercial Z-cut lithium niobate wafers by polishing the edges into a spheroidal profile. Different coupling conditions could be obtained by laterally displacing the disk from the waveguide center, getting a maximum resonance contrast of 33%. Intrinsic disk Q factor of  $1.3 \times 10^8$  was measured from resonance linewidth and confirmed by ringdown tests. The implementation of a robust planar coupling to high-Q crystalline resonators represents a crucial step toward practical applications of WGM resonators.

## Acknowledgments

Funding from Aramos project under contract Contract No B-0236-IAP1-ERG is gratefully acknowledged.